Korean J. Chem. Eng., 33(9), 2650-2658 (2016)
DOI: 10.1007/s11814-016-0127-1

pISSN: 0256-1115
eISSN: 1975-7220

Modeling and simulation of *Bacillus cereus* chitosanase activity during purification using expanded bed chromatography

Carlos Eduardo de Araújo Padilha, Nathália Kelly de Araújo, Domingos Fabiano de Santana Souza, Jackson Araújo de Oliveira, Gorete Ribeiro de Macedo, and Everaldo Silvino dos Santos†

Biochemical Engineering Laboratory, Chemical Engineering Department,
Federal University of Rio Grande do Norte (UFRN), Natal-RN, Brazil
(*Received 28 March 2016 • accepted 2 May 2016*)

Abstract−A phenomenological model was used to describe sequentially the three steps (flowthrough, washing and elution) of expanded bed adsorption chromatography for recovery of chitosanases from *Bacillus cereus*. Additionally, a hybrid strategy for model parameter estimation was carried out using particle swarm optimization and Gauss-Newton algorithms. The model was validated with independent experimental data and the statistical criteria (χ^2 and mean squared error tests) showed that the hybrid strategy was more promising than just the heuristic method. With the calibrated model, surface response methodology was applied to obtain the optimal operational conditions, and experiments were performed to confirm these results. Overall, a value of 41.08% for yield was obtained using 700 mM NaCl during elution. In summary, all approach employed in this work was relevant for maximizing the yield of the chromatographic process.

Keywords: Modeling, Expanded Bed Adsorption, Chitosanases, Particle Swarm Optimization, Gauss-Newton, Optimization

INTRODUCTION

Chitosanases endo-(3.2.1.132, Chitosan N-acetylglucosaminohydrolase) and exo-(3.2.1.165, exo-1,4-β-D-glucosaminidase) are enzymes able to hydrolyze chitosan in a specific fashion unlike other enzymes, such as common carbohydrases, lipases and proteases. They have drawn attention recently mainly for their use in many fields [1]. Among them it can be cited in the production of bioactive chitooligossacharides (COS) [2,3] as well as preparation of fungal protoplasts [4]. For instance, chitooligossacharides (pentamers to heptamers) have biological activities such as antitumor [5,6] as well as antibacterial and antifungal properties [7,8]. A rational use of these enzymes in order to obtain such COS implies on at least one purification step as it will be the case of using them immobilized onto a natural or polymer-based support. However, downstream processing (DSP), i.e., the unit operations necessary to achieve a certain purification degree, accounts for up to 50% of total cost [9] or maybe more depending on the process [10]. Therefore, DSP techniques that allow integration and intensification play important roles. In this context, expanded bed adsorption (EBA) has emerged as a powerful technique in DSP, mainly because it combines clarification, concentration and primary purification into a one step-operation [11-14]. On the other hand, mathematical models have been used in EBA studies to optimize operational conditions or even to improve the knowledge of the adsorption/desorption performance [15-19]. However, most of these works have used model proteins as well as exploiting mainly the adsorption step [15-18]. Also, with respect to modeling of this process, many works have given attention just to calculating the breakthrough curves. We highlight that, to the best of our knowledge, there is only on report [20] dealing with the modeling of the whole EBA process, that is, accounting for the three steps (adsorption-washing-elution). However, even this work used a model protein (BSA) with cell (yeast) suspension as feedstock. Of course, the whole EBA system modeling is more complex, since during elution, for instance, when ion exchange is used, it is necessary to account for the salt impact on the enzyme/protein isotherm. Therefore, a model such as steric mass action plays a key role, as can be seen in [21-24]. However, since during EBA protocol to purify an enzyme usually is needed to handle feedstock containing cells or debris and also since the target-enzyme is not purified yet, therefore the isotherm study accounting for the salt influence is hampered. To circumvent this problem it is possible to include an exponential term due to the salt concentration in the Langmuir isotherm model as carried out by [25,26]. In summary, the literature does not show many studies dealing with the whole EBA process, mainly for enzymes unclarified feedstock.

In this context, the aim of this study was to model the whole EBA process, by using a simplified general rate model, during the purification of a chitosanase produced by *Bacillus cereus* using an anionic expanded bed adsorbent. A hybrid approach coupled to statistics metrics was used to estimate the parameters of the model as well as to assess the model performance. After model validation, an optimization route was used to maximize the yield by manipulat-

†To whom correspondence should be addressed.
E-mail: everaldo@eq.ufrn.br

ing the operational conditions of the EBA process.

MATERIAL AND METHODS

1. Materials

Chitosan (85% deacetylated; molecular weight: 90-190 kDa) acquired from Sigma-Aldrich Co. (Saint Louis, USA) was solubilized using 0.1 M HCl [3]. Streamline DEAE resin was purchased from GE healthcare (Uppsala, Sweden). Buffer solutions and other chemicals were reagent grade and were used as supplied.

2. Microorganism

The microorganism used in this study was isolated from soil e identified by 16S rDNA partial nucleotide sequence analysis as shown in [27]. It consisted of a strain of *Bacillus cereus* C-01. The nucleotide sequence was deposited at GenBank (GenBank accession number SUB1125567 Seq KT875350).

3. Chitosanases Production

Aliquots of cell stocked onto nutrient agar were transferred to 50 mL of medium of preculture dispensed into 250 mL Erlenmeyer flasks. Next, they were incubated (Tecnal, TE421 - Brazil) at 120 rpm at 30 °C for 30 h. The cultivation medium was the same of preculture and consisted of ($g \cdot L^{-1}$): peptone 6.0, chitosan 2.0, magnesium sulfate 0.5 and potassium phosphate dibasic 1.0. Cultivation was carried out using 50 mL of the medium inoculated with 10% (v/v) of inoculum into 250 mL Erlenmeyer flasks [3]. Followed, the flasks were incubated at 120 rpm at 30 °C for 24 h. The culture broth was used for further purification by using EBA.

4. Experiments using EBA Chromatography

The streamline anionic exchanger resin containing the ligand Diethylaminoethyl (DEAE) and a homemade EBA column (2.6 cm×30.0 cm) were used in EBA experiments. To enhance fluid distribution at the column inlet, glass microspheres were added; therefore, the beads worked as a distributor with different bed height as shown in Table 1. A peristaltic pump (model Perimax 12, Spetec) was used to pump the feedstock through the column. Table 1 shows the experiment conditions during the EBA process. The vertical alignment of the column was guaranteed in all assays. All experiments were performed at room temperature.

The column with a given settled-bed height of resin, according to Table 1, was equilibrated with Tris-HCl (50 mM, pH 8.5) (buffer A) to give a stable expansion degree of H/H_0=1.5. 100 mL of feedstock containing cell was then loaded (flow-through step) onto column at superficial velocity according to Table 1. Next, a washing step was carried out using buffer A (150 mL). Elution was by step-wise gradient mode with Tris-HCl buffer (50 mM, pH 8.5) containing 0.3 M (buffer B), 0.7 M (buffer C), and 1 M (buffer D) NaCl. Washing and elution were conducted at the superficial velocity of 100 $cm \cdot h^{-1}$. During the three steps, fractions were collected for enzyme assay.

5. Quantification of Enzyme Activity

The chitosanolytic activity was measured by using 250 μL of enzyme sample incubated with 250 μL of 1% soluble chitosan (pH 6.0), according to [3]. The mixture was heated in a water bath for 30 minutes at 55 °C. The reaction was interrupted by boiling the samples for 10 minutes. Reducing sugars content was assayed by the 3,5-Dinitrosalicylic acid method using a spectrophotometer (Thermo Spectronic) as well as D-glucosamine as standard [3,27-30]. A unit (U) of chitosanase was defined as the amount of enzyme capable of generating 1.0 μmol of D-glucosamine per minute under the conditions described above.

MODEL FORMULATION AND OPTIMIZATION METHOD

This section addresses important considerations taken during the development of mechanistic model, concerning parameter estimation as well as optimization of the whole process EBA during the chitosanase purification. Fig. 1 shows a flowchart that outlines the present study.

First, a heuristic search over the parameters of the model for the three steps of EBA chromatography was performed by particle swarm optimization (PSO) routine. Next, parameters were identified taking the re-estimate of the most important parameters by using the Estima routine [31] that is based on the Gauss-Newton algorithm. To maximize the output variable yield (%), surface response methodology was used together with the validated model to find the best combination for the four independent variables: settled bed height, distributor settled height, superficial velocity and raw extract initial activity.

1. Mathematical Modeling of EBA Process

The mathematical modeling of the whole EBA process for the chitosanase activity into the streamline DEAE adsorbent was based on the following hypothesis:

i. Adsorbent particles are spherical with uniform density containing functional groups equally distributed on the particle surface. Correlations used to estimate the particle size ($R_p(z)$) and bed porosity ($\varepsilon(z)$) axial variation are based on [32].

ii. The hydrodynamic behavior of the fluid phase is described

Table 1. Operational conditions during chitosanase purification using EBA chromatography

Run	Settled bed height (cm)	Distributor bed height (cm)	Superficial velocity ($cm \cdot h^{-1}$)	Raw extract enzymatic activity ($U \cdot mL^{-1}$)
1	8.00	2.00	100.00	0.440
2	4.00	2.00	200.00	0.430
3	8.00	6.00	100.00	0.210
4	8.00	6.00	200.00	0.298
5[a]	6.00	4.00	150.00	0.298

[a]This run was used for mathematical model validation

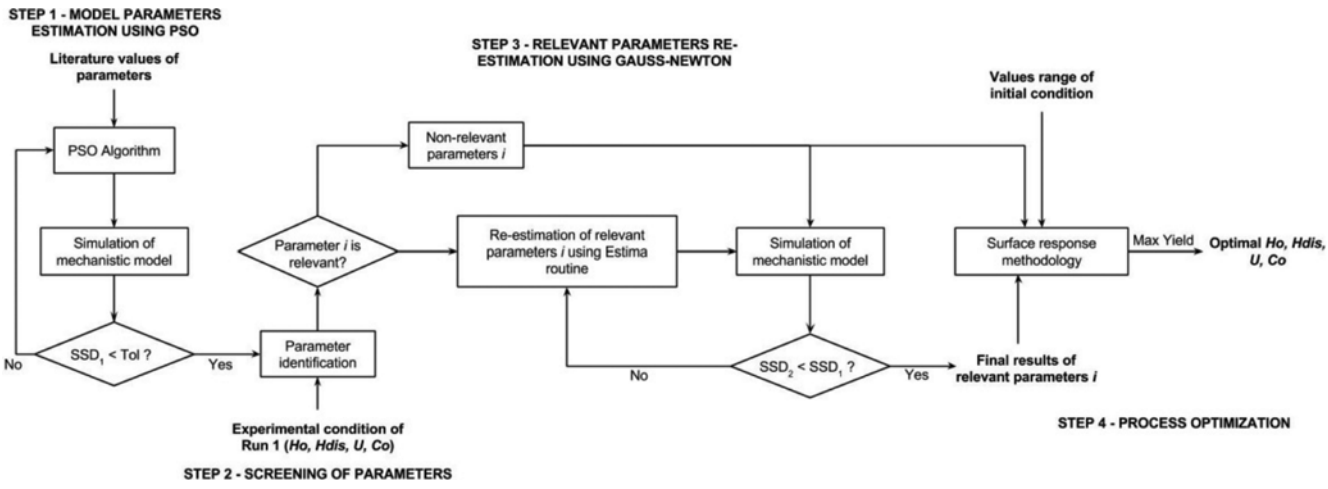

Fig. 1. Outline showing all steps developed in this study.

by axial dispersion model [16,19].

iii. The chitosanase component adsorption (1) only occurs at adsorbent surface, i.e., no internal diffusion was considered [33-36].

iv. The interaction between biomass and particles in the bed was neglected.

v. Fluid phase rheological behavior is different in each step during EBA process. Therefore, to describe the whole EBA process we included the salt component (2) during the elution step. Also, we assumed that there was no interaction between salt and adsorbent.

vi. The Langmuir modified isotherm was used to describe the adsorption equilibrium for chitosanase during the three steps of EBA process.

Eq. (1) represents the mass balance for the component i in the fluid phase:

$$\frac{\partial C_i}{\partial t} = D_{ax,\,i}\cdot\frac{\partial^2 C_i}{\partial z^2} - \frac{u}{\varepsilon(z)}\cdot\frac{\partial C_i}{\partial z} - \frac{3\cdot k_{f,\,i}\cdot(1-\varepsilon(z))\cdot(C_i - C_{i,\,R_p})}{\varepsilon(z)\cdot R_p(z)} \quad (1)$$

where $D_{ax,i}$ is the axial dispersion coefficient of component i ($cm^2\cdot s^{-1}$), $k_{f,i}$ is the film mass transfer coefficient of component i ($cm\cdot s^{-1}$), u is the superficial velocity ($cm\cdot s^{-1}$), t is the time (s), C_i and C_{i,R_p} is the concentration of component i in the fluid phase and in the particle adsorbent surface, respectively.

Initial condition (IC) and boundary conditions (BC) for the breakthrough curve are given in Eq. (1a) and Eq. (1b), respectively:

$$\text{IC: } t=0,\ C_i(z,0)=0 \quad (1a)$$

$$\text{BC: } t>0,\ z=0,\ C_i=C_{i0} \quad (1b)$$

$$z=H,\ \frac{\partial C_i}{\partial z}=0$$

Assuming that all mass transfer resistance is given by the ratio between the adsorption constant (b_1) and the desorption constant (b_2), the solid phase mass balance for the chitosanase is given by Eq. (2):

$$\frac{\partial q}{\partial t} = b_1\cdot C_1\cdot(q_{max}-q) - b_2\cdot q \quad (2)$$

where q is the chitosanase concentration adsorbed onto the solid phase and q_{max} is the maximum chitosanase adsorption capacity of the adsorbent. The initial condition for the solid phase during breakthrough step is given by Eq. (2a):

$$\text{IC: } t=0,\ q(z,0)=0 \quad (2a)$$

As recovery of the chitosanase occurs during the elution step, the term q_{max} is considered inversely proportional to the salt concentration in the fluid phase for a given column stage, as shown in Eq. (3).

$$q_{max} = q'_{max}\cdot\exp(-k_1\cdot C_2) \quad (3)$$

Assuming that the adsorption rate of the chitosanase onto the adsorbent is equivalent to the decrease of its concentration in the fluid phase the term C_{i,R_p} (Eq. (4)) can be obtained through mathematical manipulation of Eqs. (1) and (2). As the salt component has no solid balance equation then $C_{2,R_p}=C_2$ such that the third term in the Eq. (1) becomes null.

$$C_{1,\,R_p} = C_1\left(1+\frac{R_p(z)b_1q_{max}}{3k_{f,\,1}}\right) - \frac{R_p(z)q}{3k_{f,\,1}}(b_1C_1+b_2) \quad (4)$$

Eqs. (1-4) can also be used to describe the washing ($C_{10}=0$, $C_{20}=0$) and elution ($C_{10}=0$, $C_{20}>0$) steps, except for the two initial conditions, given by Eqs. (1a) and (2a), that should correspond to the final of the loading and washing steps, respectively. Each step has its own parameter dataset for chitosanase, but the values of q_{max}, b_1 and b_2 were fixed, giving 11 parameters overall. The subscripts *l*, w and e were used to clarify the parameters belonging to the loading, washing and elution, respectively.

The mathematical model of the general rate was written in Fortran 90, in the Microsoft Visual Studio platform. The method of lines was used for numerical integration of the model during all steps [37]. In this method the chromatography column height (z space coordinate) was discretized in 30 elements using the central finite difference method. To each element, the partial time derivative was approximated by an ordinary derivative. The resultant system of ordinary differential equations discretized for the n elements was solved using the DASSL numerical route [38].

2. Estimation of the Model Parameters

The model parameters were estimated by using the particle swarm

optimization (PSO) algorithm. This is a heuristic search algorithm inspired by social behavior of bird flocking or fish schooling. The estimation is carried out by a population of potential solutions called particles. The particles move in a multidimensional space exchanging information with each other over the objective function (OF) [33-36]. The OF to be minimized is type weighted minimum mean square then relating the experimental (C_i^{exp}) and calculated (C_i^{calc}) difference associated with square standard deviation (σ_i) as shown in Eq. (5).

$$OF = \sum_{i=1}^{N} \frac{(C_i^{exp} - C_i^{calc})^2}{\sigma_i^2} \quad (5)$$

In this study we used 20 particles and 20 iterations as values for the initial, cognitive and social parameters fixed in 0.7, 1.0 and 1.0, respectively. The intervals of search for the model parameters were: $D_{ax,1l}$, $D_{ax,1w}$, $D_{ax,2} \in [5\times10^{-3}, 0.75]$ $cm^2\cdot s^{-1}$, $k_{f,1l}$, $k_{f,1w} \in [5\times10^{-3}, 0.75]$ $cm\cdot s^{-1}$, $q_{max} \in [0.3, 1.2]$ $U\cdot mL^{-1}$, $b_1 \in [10^{-2}, 0.5]$ $g\cdot U^{-1}\cdot s \in^1$, $b_2 \in [5\times10^{-4}, 5\times10^{-2}]$ s^{-1}, $D_{ax,1e} \in [5\times10^{-5}, 2.5\times10^{-3}]$ $cm^2\cdot s^{-1}$, $k_{f,1e} \in [5\times10^{-5}, 5\times10^{-2}]$ $cm\cdot s^{-1}$, $k_1 \in [5\times10^{-3}, 0.75]$ $L\cdot mmol^{-1}$. As the whole EBA process consists of loading, washing and elution steps, there was a simultaneous estimation of model parameters. After PSO, we did a parametric sensibility assay. Some parameters were re-estimated by the Gauss-Newton algorithm. In this case, Estima was used to minimize the OF as described by Eq. (5). Therefore, using this package it was also possible to obtain the matrix of covariance and standard deviations of the parameters of the model.

3. Optimization of the Chitosanase Yield During EBA Chromatography

The main advantage of using mathematical modeling is that one can simulate the process using experimental conditions yet not tested based on the set of estimated parameters [33]. Then, this section was considered to evaluate the effect of the initial load concentration, settled bed height, distributor settled bed height as well as superficial velocity over the chitosanase yield during the EBA. The objective function to be maximized is the elution yield at 700 mM NaCl as shown in Eq. (6):

$$\text{Yield}\ (\%) = \frac{\left(\int_{t_{e1}}^{t_{e2}} (C_1 \cdot dt)\right)\cdot F}{C_{10}\cdot V_{loading}} \cdot 100 \quad (6)$$

where the integration multiplied by F results in the eluted quantity of chitosanase at 700 mM NaCl, F is the volumetric flow-rate and $V_{loading}$ is the volume of load of the raw extract containing chitosanase fed to the column (C_{10} in Eq. (6)). To know the most important parameters influencing the yield of chitosanase activity, we used SRM. In this case, the input variables were C_{10}, H_0, H_{dis} as well u. The range used was the same shown in Table 1: the same as the calibration step. This assay was performed using STATISTICA 7.0 software (StatSoft, USA).

RESULTS AND DISCUSSION

We modeled the whole EBA process during the purification of a chitosanase produced by *Bacillus cereus* using an anionic expanded bed adsorbent. In the case of super-parameterized systems, as the one assayed in present study, the model can contain non-identifiable parameters, then limiting the method based on gradients [39]. Therefore, we have applied a strategy of hybrid parametric estimation. In this case, it was taken as the initial values of deterministic method the set of parameters estimated by the heuristic method. Due to its own advantageous characteristics the PSO algorithm was used to perform the estimation of 11 parameters of the model. In this case, experimental data from runs 1 to 4 were used. The estimated values for the PSO algorithm are shown in Table 2.

Table 2. Model estimated parameters obtained by the PSO algorithm and for the Gauss-Newton algorithm using the computational package Estima

Parameter	PSO algorithm	Re-estimation using Gauss-Newton algorithm
$D_{ax,1l}$ ($cm^2\cdot s^{-1}$)	1.065×10^{-2}	$1.144\times10^{-2}\pm1.441\times10^{-3}$
$k_{f,1l}$ ($cm\cdot s^{-1}$)	0.430	0.430
q_{max} ($U\cdot mL^{-1}$)	0.907	$0.774\pm6.376\times10^{-2}$
b_1 ($g\cdot U^{-1}\cdot s^{-1}$)	3.134×10^{-2}	$3.345\times10^{-2}\pm4.637\times10^{-3}$
b_2 (s^{-1})	1.000×10^{-3}	$4.091\times10^{-4}\pm1.749\times10^{-4}$
$D_{ax,1w}$ ($cm^2\cdot s^{-1}$)	3.953×10^{-2}	$3.814\times10^{-2}\pm5.058\times10^{-3}$
$k_{f,1w}$ ($cm\cdot s^{-1}$)	0.474	0.474
$D_{ax,1e}$ ($cm^2\cdot s^{-1}$)	1.710×10^{-3}	1.710×10^{-3}
$k_{f,1e}$ ($cm\cdot s^{-1}$)	3.995×10^{-3}	3.995×10^{-3}
$D_{ax,2}$ ($cm^2\cdot s^{-1}$)	6.291×10^{-4}	6.291×10^{-4}
k_1 ($L\cdot mmol^{-1}$)	0.488	0.488

A parametric sensibility analysis was performed over the parameters dataset calibrated by the PSO algorithm following the methodology proposed by [40] as well as [41]. The metric for the parameter sensibility δ^{msqr} was obtained for each process step such as $\delta^{msqr}_{loading}$, $\delta^{msqr}_{washing}$, $\delta^{msqr}_{elution}$, for the loading, washing and elution, respectively. Also a global assay was performed using the indicator δ^{msqr}_{total} and a selected threshold. The parameters are positioned according to the EBA steps and are shown in Fig. 2.

The parametric sensibility results showed that the liquid axial dispersion coefficient ($D_{ax,1l}$), the maximum adsorption capacity (q_{max}) and the adsorption (b_1) and desorption (b_2) of chitosanase during the loading step as well as the liquid axial dispersion coefficient in the washing step ($D_{ax,1w}$) were the most influential parameters in the model. Therefore, changes in the liquid axial dispersion coefficient during elution ($D_{ax,1e}$), in the liquid film mass transfer coefficient for the three steps ($k_{f,1l}$, $k_{f,1w}$, $k_{f,1e}$), in the liquid axial dispersion coefficient for the salt ($D_{ax,2}$) as well as for the term of protein displacement induced by the salt presence (k_1) little affected the metric δ^{msqr}_{total} then being considered not relevant to the level of 0.15 for this reason they were fixed.

The relevant parameters can be expressed in vector form as shown in Eq. (7).

$$\theta_S = [D_{ax,1l}\ \ q_{max}\ \ b_1\ \ B_2\ \ D_{ax,1w}]^T \quad (7)$$

The parameters θ_S were re-estimated over the same dataset to obtain a better adjustment. The strategy of estimation using a unique step has also been kept. The Table 2 illustrates the obtained re-estimated parameters and their standard deviations as shown in the second column of this table.

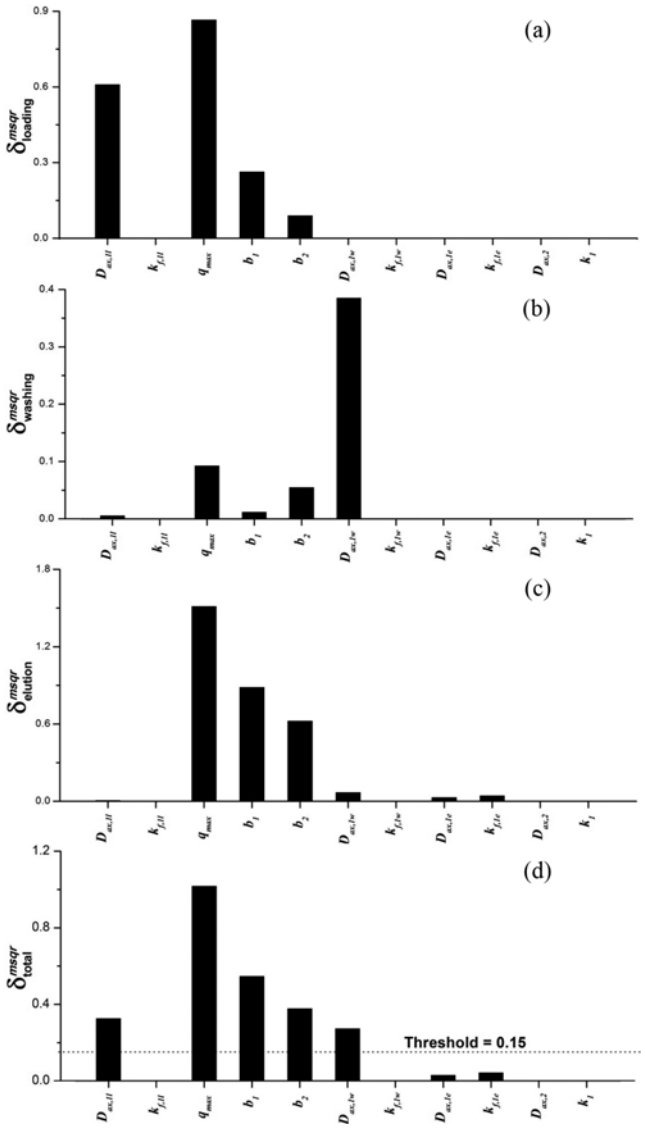

Fig. 2. Profiles for the metric δ^{msqr} for the loading ($\delta^{msqr}_{loading}$) (a), washing ($\delta^{msqr}_{washing}$) (b) and elution steps ($\delta^{msqr}_{elution}$) (c). The total sensibility metric δ^{msqr}_{total} related to the model parameters θ_k as well the threshold delimiting the relevant parameters of the model at 0.15 level (d).

Fig. 3 shows the simulated profiles for the chitosanase activity concentration at the column exit during the EBA process at different operational condition using the estimated parameters for the PSO and Gauss-Newton algorithms. The value difference among the five terms of θ_S altered significantly the model behavior during the three steps. The breakthrough curves built used the PSO algorithm, even though showing the characteristic S shape is displaced to the right while the breakthrough curves built using the re-estimated parameters showed saturation in advance as well as reaching super-estimated values for the activity concentration at column exit. During the washing step is evident the best performance showed by the re-estimated parameters compared to the parameters fitted by the PSO algorithm. The inclusion of the exponential term in the Langmuir equation in fact improved the elution profile, allowing a description of this step during the EBA process modeling. Therefore, this strategy showed successful to model the chitosanase activity concentration. It can be seen that for the elution carried out using 700 mM NaCl, the simulated peaks generated using the parameters estimated by the PSO algorithm showed higher efficiency than those generated by the Gauss-Newton algorithm. However, since the experimental peaks during chitosanase elution using an anionic adsorbent manufactured and are used in EBA process showed larger peaks, the latter showed better adjustment of the chitosanase activity concentration elution profile.

Also, regardless of the parametric dataset used, there was a larger deviation between the experimental and simulated results during the elution step using 300 mM NaCl. In this case, a lower degree of chitosanase activity concentration was registered at the column exit. This fact can be possibly explained due to the decrease in the bed porosity during the regime change when the bed was operated packed, during elution, instead of expanded, during washing. Then, this fact seems to have contributed to the desorption for chitosanase in the simulations, but it is in disagreement with the experimental observations.

The quality of the simulated curve adjustment concerned to experimental data was determined using the χ^2 test as well as the mean square error (MSE), as shown in Eq. (8) and Eq. (9), respectively.

$$\chi^2 = \frac{\sum_{i=1}^{N}(C_{1i,\,exp} - C_{1i,\,calc})^2}{C_{1i,\,calc}} \tag{8}$$

$$MSE = \frac{\sum_{i=1}^{N}(C_{1i,\,exp} - C_{1i,\,calc})^2}{N} \tag{9}$$

Table 3 illustrates the values for both χ^2 and MSE obtained in the calibration as well as validation runs for the parametric data of PSO and Gauss-Newton algorithms. Concerning the runs used for parameter calibration, we observed that the PSO parameter set showed lower values for both χ^2 and MSE, then having the equality hypothesis been accepted for the four runs at the 95% confidence level and freedom degree of 41 (χ^2_c=56.94). The re-estimation of the θ_S parameters only allowed the increasing of the global quality adjustment. However, we observed an increment of the MSE during the run 2 simulation. Also, good results were obtained for the run 5 simulation even thought this run wasout of the data used for the model estimation. The re-estimation for the parameters by the Gauss-Newton algorithm reduced the MSE value from 9.634×10^{-4} to 8.671×10^{-4} as well as the χ^2 value from 0.90 to 0.88. Then, this result shows that hybrid estimation is a quite interesting way for general rate model parameter estimation.

Since the model was validated, it has been used to optimize the operational conditions for the EBA process, taking as the objective function the yield during elution with 700 mM NaCl as described by Eq. (6). In this case, the values of volumes used during loading, washing and elution, the flow-rate for elution as well as the salt concentrations for the elution solutions were kept unaltered. The effects of H_0, C_{10} as well u over the yield can be observed by the surface response plots, as shown in Fig. 4. It can be seen observed

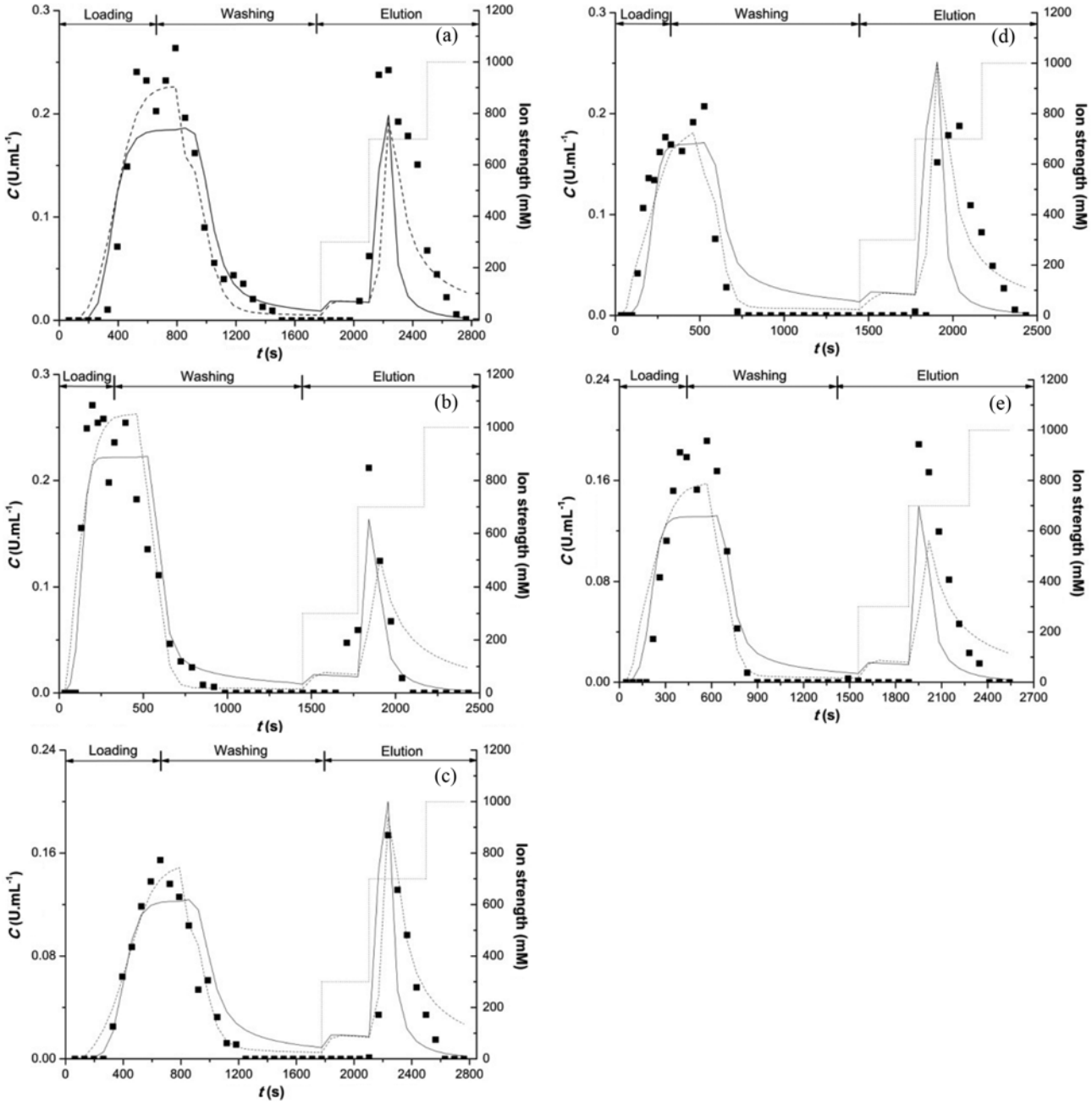

Fig. 3. Profiles of the chromatograms for the chitosanase activity concentration during a whole EBA process simulation. (a) Run 1; (b) Run 2; (c) Run 3; (d)- Run 4; (e) Run 5*. (■) experimental data. The solid line is the simulation using the model parameter estimated by the PSO. The dashed line is the simulation using re-estimated parameters. * This run was used to validate the model. The dotted line is the salt concentration during elution.

Table 3. Values for the statistical metrics χ^2 and MSE obtained during model simulation using the parameter data obtained by the PSO and Gauss-Newton algorithms

Parameter set		Run 1	Run 2	Run 3	Run 4	Run 5
Without re-estimation	χ^2	3.98*	9.77*	0.97*	4.19*	0.90*
	MSE	2.560×10^{-3}	8.364×10^{-4}	9.215×10^{-4}	3.258×10^{-3}	9.634×10^{-4}
With re-estimation	χ^2	1.49*	3.68*	0.33*	0.59*	0.88*
	MSE	1.800×10^{-3}	1.699×10^{-3}	2.327×10^{-4}	9.497×10^{-4}	8.671×10^{-4}

*Significant parameter at 95% confidence level

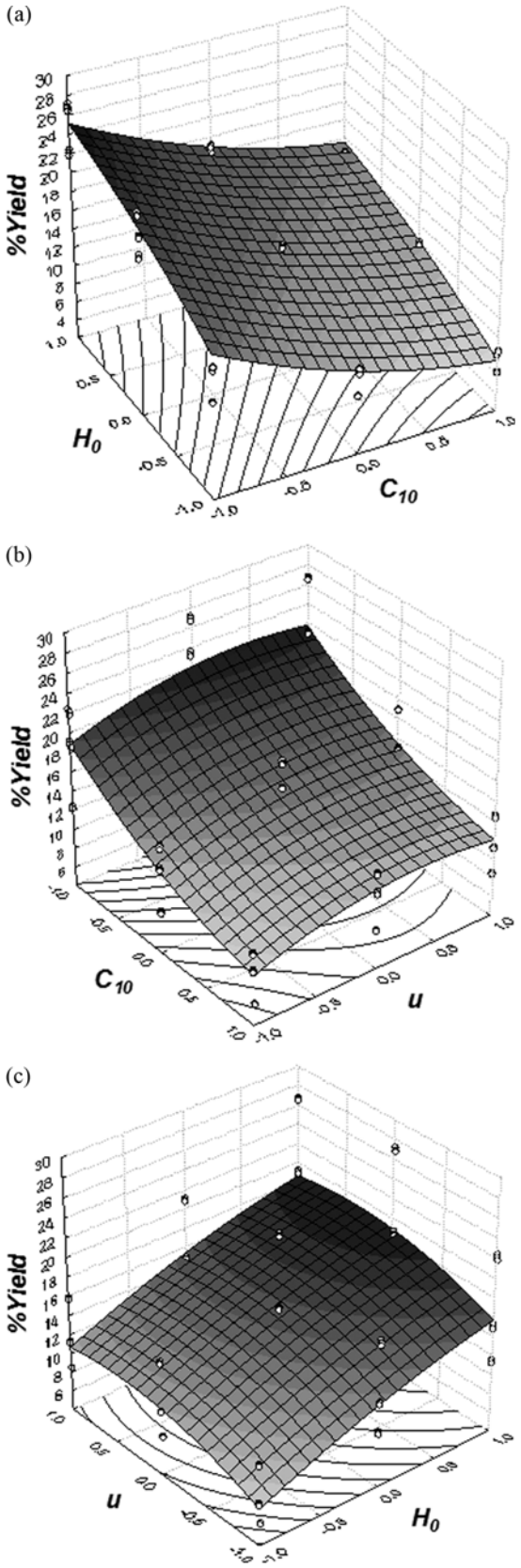

Fig. 4. Response surface for the chitosanase activity yield considering the effect of two operational conditions on the yield (considering the others at central condition). (a) H_0 and C_{10}, (b) C_{10} and u, (c) H_0 and u.

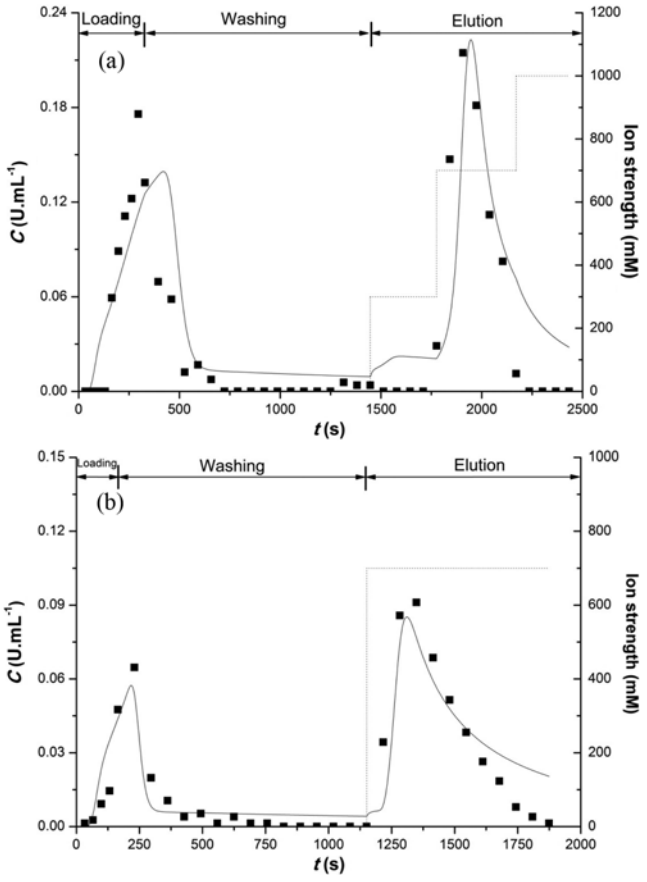

Fig. 5. Profiles of the chromatograms for the chitosanase activity concentration during a whole EBA process under optimal operational conditions obtained by SRM (a) and modified conditions (b). (■) experimental data. The solid line is the model simulation using the re-estimated parameters. The dotted line is the salt concentration during elution.

that the yield is improved by the increase of the both H_0 and u being reduced with the increase of C_{10}. This result is based on the fact that a higher H_0 implies more adsorbent in the bed as well as a lower occurrence of back-mixing, i.e., mainly due to distributor effect; also, the increase in the velocity favors mass transfer. The reduction of the yield due to the increase of C_{10} can be explained mainly for the possibility of the competitive adsorption by the contaminants. It was observed that H_{dis} has no effect on the yield. Therefore, these three parameters are important to increase the purification yield.

The optimization using RSM showed that the best operational condition to maximize the yield was H_0=8 cm, H_{dis}=2 cm, u=200 cm/h and C_{10}=0.21 U/mL. Fig. 5(a) shows the chromatogram with the experimental as well as the simulated data for the optimized conditions during the EBA process. In this case, using elution with 700 mM NaCl we obtained a maximum yield of 26.78% for the model. We highlight that this yield shows good agreement with the experimental one (29.42%) considering the same conditions. Also, this value is higher than the yield obtained for the same step (elution with 700 mM NaCl) during run 4 (22.28%) as shown in Fig. 3(d), i.e., the run showing the highest yield during the calibra-

tion step.

Since the overall enzyme yield obtained using the stepwise elution with 700 mM NaCl was quite low, therefore, to improve this parameter as well as to reduce the operation time during EBA process, a validation experiment was conducted mainly changing two operational conditions: the feedstock volume was reduced from 150 mL to 50 mL and also elution mode was changed to isocratic (700 mL NaCl) instead of stepwise (300, 700 and 1,000 mM NaCl). As can be seen in Fig. 5(b), this new strategy to the optimum conditions for MSE reduced proportionally the loss of adsorbate during the flow through, since the term C/C_0 in this step was lower than 0.25, like most industrial approaches. Besides, since the stepwise mode was not considered during the elution step, all activity recovered was taken for the calculation of the yield using the EBA process. The model also showed good prediction performance, showing yield of 41.08%, which is quite similar to the value obtained for the experiment (40.67%).

CONCLUSION

A mathematical model was used to describe the whole EBA process during the chitosanase purification protocol. A hybrid approach, using both the PSO and Gauss-Newton algorithm, was used to the model parameter estimation coupled to a parametric sensibility assay. The re-estimation improved the mathematical model performance, mainly concerning the relevant parameters such as $D_{ax,1b}$, q_{max}, b_1, b_2 and $D_{ax,1w}$. Overall, this model adjusted quite well the whole EBA process. Also, using the optimized condition it is possible to reach 41.08% maximum yield using 700 mM NaCl elution. The results showed that the strategy of using an exponential term to model the elution as well as a simplified equilibrium condition steps during EBA process is successful.

NOMENCLATURE

b_1 : adsorption constant of modified Langmuir isotherm [L/U·s]
b_2 : desorption constant of modified Langmuir isotherm [1/s]
C_{i0} : initial concentration of component i in the fluid phase [U/mL]
C_i : concentration of component i in the fluid phase [U/mL]
C_{i,R_p} : concentration of component i in the particle adsorbent surface [U/mL]
$D_{ax,i}$: axial dispersion coefficient of component i [cm^2/s]
F : volumetric flow-rate [cm^3/s]
H_0 : fixed bed height [cm]
H : expanded bed height [cm]
k_1 : exponential term of modified Langmuir isotherm [mM^{-1}]
$k_{f,i}$: film mass transfer coefficient of component i [cm/s]
MSE : mean square error
N : number of experimental data
OF : objective function
PSO : particle swarm optimization
q : chitosanase concentration adsorbed onto the solid phase [U/mL_{ads}]
q_{max} : maximum chitosanase adsorption capacity of the adsorbent [U/mL_{ads}]
R_p : particle adsorbent size [cm]
t : time [s]
u : superficial velocity [cm/s]
$V_{loading}$: loading volume [mL]
z : axial dimension [cm]

Greek Letters

δ^{msqr} : parameter sensibility
E : bed porosity
θ_S : relevant model parameters
Σ : square standard deviation
χ^2 : reduced square chi
χ_c^2 : critical reduced square chi

ACKNOWLEDGEMENTS

The authors thank CAPES and Brazilian National Council of Research (CNPq) for the financial support.

REFERENCES

1. N. Thadathil and S. P. Velappan, *Food Chem.*, **150**, 392 (2014).
2. S. L. Wang, W. N. Tseng and T. W. Liang, *Biodegradation*, **22**, 939 (2011).
3. N. K. Araujo, C. F. Assis, E. S. Santos, G. R. Macedo, L. F. Farias, H. Arimateia Jr., M. F. F. Pedrosa and M. G. Pagnoncelli, *Appl. Biochem. Biotechnol.*, **170**, 292 (2013).
4. S. K. Hsu, Y. C. Chung, C. T. Chang and H. Y. Sung, *J. Agric. Food Chem.*, **60**, 649 (2012).
5. C. F. Assis, L. S. Costa, R. F. Melo-Silveira, R. M. Oliveira, M. G. Pagnoncelli, H. A. Rocha, G. R. Macedo and E. S. Santos, *World J. Microb. Biotechnol.*, **28**, 1097 (2012).
6. S. Masuda, K. Azuma, S. Kurozumi, M. Kiyose, T. Osaki, T. Tsuka, N. Itoh, T. Imagawa, S. Minami, K. Sato and Y. Okamoto, *Carbohydr. Polym.*, **111**, 783 (2014).
7. S. J. Wu, S. K. Pan, H. B. Wang and J. H. Wu, *Int. J. Biol. Macromol.*, **62**, 348 (2013).
8. I. Younes, S. Sellimi, M. Rinaudo, K. Jellouli and M. Nasri, *Int. J. Food Microb.*, **185**, 57 (2014).
9. E. S. Santos, R. Guirardello and T. T. Franco, *J. Chromatogr. A*, **944**, 217 (2002).
10. R. N. D'Souza, A. M. Azevedo, M. R. Aires-Barros, N. L. Krajnc, P. Kramberger, M. L. Carbajal, M. Graselli, R. Meyer and M. Fernández-Lahore, *Pharm. Bioprocess.*, **1**, 423 (2013).
11. C. J. Fee, *Chem. Eng. and Processing: Process Intensif.*, **40**, 329 (2001).
12. A. Ramos, F. G. Acien, J. M. Fernandez-Sevilla, C. V. Gonzalez and R. Bermejo, *J. Chromatogr. B*, **879**, 511 (2011).
13. V. Boeris, I. Balce, R. R. Vennapusa, M. Arevalo Rodriguez, G. Pico and M. Fernández-Lahore, *J. Chromatogr. B*, **900**, 32 (2012).
14. F. C. Sousa Junior, M. R. F. Vaz, C. E. A. Padilha, A. S. Chibério, D. R. A. Martins, G. R. Macedo and E. S. Santos, *J. Chromatogr. B*, **986**, 1 (2015).
15. P. R. Wright and B. J. Glasser, *AIChE J.*, **47**, 474 (2001).
16. X. D. Tong, B. Xue and Y. Sun, *Biochemic. Eng. J.*, **16**, 265 (2003).
17. P. Li, G. Xiu and A. E. Rodrigues, *AIChE J.*, **51**, 2965 (2005).
18. J. Yun, D. Q. Lin and S. J. Yao, *J. Chromatogr. A*, **1095**, 16 (2005).

19. C. E. A. Padilha, D. F. S. Souza, J. A. Oliveira, G. R. Macedo and E. S. Santos. *Current Chromatogr.*, 3, **44** (2016).
20. W. D. Chen, X. Y. Dong and Y. Sun. *J. Chromatogr. A*, **1012**, 1 (2003).
21. W. Li, S. Zhang and Y. Sun, *Biochem. Eng. J.*, **22**, 63 (2004).
22. A. Osberghaus, S. Hepbildikler, S. Nath, M. Haindl, E. von Lieres and J. Hubbuch, *J. Chromatogr. A*, **1237**, 86 (2012).
23. F. Dismer, S. Hansen, S. A. Oelmeier and J. Hubbuch, *Biotechnol. Bioeng.*, **110**, 683 (2013).
24. A. Osberghaus, S. Hepbildikler, S. Nath, M. Haindl, E. von Lieres and J. Hubbuch, *J. Chromatogr. A*, **1233**, 54 (2012).
25. F. D. Antia and C. Horváth, *J. Chromatogr. A*, **484**, 1 (1989).
26. J. Chen and Y. Sun, *J. Chromatogr. A*, **992**, 29 (2003).
27. N. K. Araújo, M. G. B. Pagnoncelli, V. C. Pimentel, M. L. O. Xavier, C. E. A. Padilha, G. R. Macedo and E. S. Santos, *Int. J. Biol. Macromol.*, **82**, 291 (2016).
28. C. C. Assis, N. K. Araujo, M. G. B. Pagnoncelli, M. R. S. Pedrini, G. R. Macedo and E. S. Santos, *Bioprocess Biosyst. Eng.*, **33**, 893 (2010).
29. S. C. Santana, R. C. Silva Filho, J. S. Cavalcanti, J. A. Oliveira, G. R. Macedo, F. F. Padilha and E. S. Santos, *Korean J. Chem. Eng.*, **31**, 684 (2014).
30. S. C. Santana, R. C. Silva Filho, J. S. Cavalcanti, J. A. Oliveira, G. R. Macedo, F. F. Padilha and E. S. Santos, *Biocatal. Agric. Biotechnol.*, **4**, 727 (2015).
31. F. B. Noronha, J. C. Pinto, J. L. Monteiro, M. W. Lobão and T. J. Santos, Estima - Pacote Computacional para Estimação de Parâmetros e Projeto de Experimentos, *PEQ Internal Report* (1993).
32. P. Li, G. Xiu and A. E. Rodrigues, *AIChE J.*, **51**, 2965 (2005).
33. C. C. Moraes, M. A. Mazutti, M. I. Rodrigues, F. Maugeri Filho and S. J. Kalil, *J. Chromatogr. A*, **1216**, 4395 (2009).
34. C. A. V. Burkert, G. N. O. Barbosa, M. A. Mazutti and F. Maugeri Filho, *Process Biochem.*, **46**, 1270 (2011).
35. C. C. Moraes, M. A. Mazutti, F. Maugeri Filho and S. J. Kalil, *J. Chromatogr. A*, **1281**, 73 (2013).
36. F. C. Sousa Jr., C. E. A. Padilha, A. S. Chibério, V. T. Ribeiro, D. R. A. Martins, J. A. Oliveira, G. R. Macedo, E. S. Santos, *Sep. Purif. Technol.*, **164**, 34 (2016).
37. M. E. Davis, Numerical Methods and Modeling for Chemical Engineers, Wiley, New York (1984).
38. L. R. Petzold, DASSL code, version 1989, Computing and Mathematics Research Division, Lawrence Livermore National Laboratory, L316, PO Box 808, Livermore, CA 94559 (1989).
39. P. C. Giordano, A. J. Beccaria, H. C. Goicoechea and A. C. Olivieri, *Biochem. Eng. J.*, **80**, 1 (2013).
40. R. Brun, P. Reichert and H. R. Künsch, *Water Resour. Res.*, **37**, 1015 (2001).
41. R. M. Prunescu and G. Sin, *Bioresour. Technol.*, **150**, 393 (2013).